Configurational bias Monte Carlo simulation of phase segregation in block copolymer networks

Kent I. Palmer[a] and Christian M. Lastoskie[b]
Department of Chemical Engineering, Michigan State University, East Lansing, Michigan 48824

(Received 31 July 2003; accepted 9 October 2003)

Cross-linked block copolymers are used as adhesives in fiber-reinforced composite material manufactures for automotive applications. Good adhesion between the polymer matrix and fibers in the interphase region is required for the structural integrity of these materials. Experimental evidence indicates that superior adhesion is obtained when phase segregation occurs between the two matrix phase block copolymers. It is therefore desirable to predict the conditions under which phase segregation is expected to occur. Configurational bias Monte Carlo simulations of two-component, trifunctional block copolymer networks were carried out to investigate phase segregation in these materials. The effects of four principal parameters on phase segregation were examined: the weight fractions of the two components, the cross-link length, the connectivity of the network, and the ratio of the square-well interactions. The molecular simulation results confirmed trends observed in laboratory measurements. © *2004 American Institute of Physics.*
[DOI: 10.1063/1.1630792]

I. INTRODUCTION

Cross-linked polyurethanes find wide application in industry and pose an interesting challenge to the molecular modeling community due to the high-density, highly cross-linked polymers involved. Of special interest to the automotive industry are polyurethane–glass interactions. Several studies[1–4] have demonstrated that good adhesion at the interphase between the polyurethane and glass is essential to ensure overall structural integrity for various applications utilizing these composite materials. Agrawal and Drzal[5–7] synthesized polyurethanes from polycaprolactone-based triols and toluene diisocyanate, the so-called soft segment and hard segment regions, respectively, using Macosko's terminology[8] in reference to the low and high glass transition temperatures of the soft and hard segment domains. By varying the weight ratio of triol to diisocyanate, and by using triols of three different molecular weights, composite structures were produced that exhibited widely varying extents of phase segregation. Specifically, variation of hard segment/soft segment weight fraction allowed experimental investigation of the energetic effect of hydrogen bonding, while variation of the size of the triol constituent provided insight on the effect of cross-link length. Transition temperatures obtained from differential scanning calorimetry[5] revealed that higher hard segment content increased the degree of phase segregation in polyurethanes. Near-infrared spectroscopy and Fourier transform infrared spectroscopy measurements were also consistent with this finding. Tensile tests and Iosipescu shear experiments[5] further revealed that phase segregation is most pronounced for polyurethanes that were prepared from high molecular weight triols with high hard segment weight fractions.

Angular-dependent x-ray photoelectron spectroscopy (ADXPS) measurements[6] were conducted on polyurethanes adhered to glass substrates. An interphase region was detected between the glass substrate and polyurethane matrix. The composition of this interphase region was found to depend on the composition of the polyurethane matrix and the extent of phase segregation within the matrix. Surface free energies for the interphase region were calculated using the method of Eberhardt[9] with an additive function proposed by Van Krevelen.[10] Upon comparing these calculations with data obtained from block-shear measurements,[7] a linear relationship was discovered between the polar surface free energy and the strength of adhesion. The highest polar surface free energies were observed in phase-separated polyurethanes in which phase segregation had caused butanediol and butandediol-derived moieties to preferentially segregate to the polyurethane surface. On the basis of this observation, Agrawal and Drzal hypothesized that adhesion between the polyurethane and the glass surface occurs by the formation of hydrogen bonds within the butanediol-rich interphase region and the hydroxylated glass surface.[7] Therefore, by increasing the hard segment weight fraction, or by increasing the molecular weight of the triol cross-linking component, phase segregation in the polyurethane matrix can be increased, thus strengthening adhesion between the polyurethane and glass substrate and improving the overall structural integrity of composite materials manufactured from polyurethane reaction injection molding with a fibrous glass reinforcement additive.[5–7]

A number of different network simulation methods[11–32] and theoretical models[33–37] have been put forth to interpret experimental measurements or predict the properties of block

[a]Present address: General Motors Truck Group, Mail Code 483-550-310, 1999 Centerpoint Parkway, Pontiac, MI 48341-3150.
[b]Present address: Department of Civil & Environmental Engineering, University of Michigan, 178 EWRE Building, 1351 Beal Avenue, Ann Arbor, MI 48109-2125. Author to whom correspondence should be addressed. Electronic mail: cmlasto@umich.edu

copolymer-derived networks. Binder[11] reviews three types of network constructs commonly used to model cross-linked systems using molecular simulation. The first construct is a randomly linked network[12–19] created by cross linking an equilibrated melt. This type of structure most closely corresponds to radiation cross-linked or vulcanized polymers. The second type of construct is an end-linked network, in which an equilibrated monodisperse melt is kinetically cross linked at the chain ends, either by defining a certain percentage of chain ends as multifunctional sites which can bond with more than two sites[20–25] or by using cross linkers.[26,27] In an end-linked network, all the cross links and dangling chain ends have the same length, whereas in a randomly linked network there is a distribution of cross-link lengths and dangling chain lengths.

The third, and most idealized, network construct is the fully connected network[28–30] in which there are no dangling chain ends, in contrast to the random or end-linked structures. Fully connected networks have been used to study simple networks[28,29] as well as gel swelling[29,30] by the inclusion of solvent molecules in the polymer network. Lay *et al.*[15] conducted lattice-based bond-fluctuation Monte Carlo simulations on fully connected networks consisting of stochastically cross-linked diblock copolymers to investigate structural behavior based upon A–B repulsion parameters. Escobedo and de Pablo[28–30] carried out athermal and square-well isothermal–isobaric Monte Carlo simulations of a fully connected, defect-free continuum diamondlike network to investigate equation of state behavior and attractive interaction effects on polymer packing fraction. Because of the difficulties associated with equilibrating fully connected polymer networks using conventional Monte Carlo methods, Escobedo and de Pablo[28–30] developed extended continuum configurational bias (ECCB) Monte Carlo simulation methods involving cluster,[30] hole,[31] and slab[32] sampling algorithms to more efficiently sample the configuration space of fully cross-linked networks with trifunctional or tetrafunctional nodes. In general, simulations of fully connected networks have been limited to homopolymers, whereas simulations of block copolymer structures have been confined to randomly linked networks.

Flory–Huggins theory[33] is the most commonly used theoretical model for describing the properties of polymer blends.[34] In Flory–Huggins theory, the Flory interaction parameter χ describes the interaction energy between polymer chains. This parameter has been used to estimate solubility differences,[10] which are known to be an important driving force for phase segregation.[11] Phase segregation occurs when χ exceeds a critical value χ_C. The functions for χ and χ_C in Flory–Huggins theory are such that phase segregation occurs when the solubility differences are large or when the polymer chain length is large.

Agrawal and Drzal obtained χ values for polyurethane block copolymers using a group contribution method.[10] Because the Flory–Huggins model strictly applies only to polymer blends, not cross-linked polymer networks, Agrawal and Drzal referenced phase diagrams developed by Benoit and Hadziioannou[35] for multiblock copolymers to obtain estimates for χ_C and thereby predict whether phase segregation occurs in polyurethane matrices.[6] Qualitative agreement was obtained between the Flory–Huggins model predictions and experimental results from differential scanning calorimetry. Alternative modified Flory–Huggins theories, which model phase segregation as a function of transition temperature rather than polymer composition or structure, have been proposed by de Gennes[36] and Vargas and Barbosa.[37]

In this work, we present results from isobaric–isothermal (NPT) Monte Carlo (MC) simulations of diblock, trifunctional copolymer networks that mimic polyurethane matrix structures. The objectives of the simulation study are twofold. First, the effects of three principal structural parameters on the phase segregation behavior are investigated in a systematic fashion. Second, the ability of the NPT MC simulation approach to quantitatively predict phase segregation is evaluated against experimental observations and Flory-based theoretical calculations for polyurethane block copolymer networks.

II. COMPUTATIONAL METHODOLOGY

MC simulations are based on importance sampling schemes. The initial algorithm focused on small molecules,[38] but Rosenbluth and Rosenbluth[39] developed a method for longer polymer configurations. Siepman and Frenkel[40] expanded this concept by introducing a configurational bias Monte Carlo (CBMC) method to efficiently sample lattice-based polymers. De Pablo, Laso, and Suter[41] extended CBMC to continuum modeling of polymers. CBMC involves deletion of a fragment of a randomly selected polymer chain, followed by regrowth of the deleted chain fragment, site by site, into a new configuration. For polymer networks, regrowth of the deleted chain must be carried out in a manner that preserves the connectivity of the network; this is accomplished through the use of the crankshaft algorithm.[42,43] Escobedo and de Pablo[31] devised a method for thermal equilibration of networks, termed extended continuum configurational bias (ECCB) Monte Carlo, in which an arbitrary chain fragment, that may include trifunctional or tetrafunctional nodal segments, can be deleted and regrown with chain reclosure assured. For mechanical equilibration in the NPT ensemble, the ''slab'' method[32] is employed to sample the volume occupied by the polymer network, by arbitrarily selecting a thin rectangular slab of the simulation cell, increasing or decreasing its width, and then repositioning the sites within the slab so as to satisfy connectivity restraints. The simulation results reported in this work were all obtained using ECCB MC simulation with the slab algorithm to achieve rapid thermal and mechanical equilibration and satisfactory sampling of the configurational phase space of the block copolymer network structures.

The chains in the simulated networks are constructed of rigid, freely jointed spherical monomer units or ''segments.'' Each monomer has a molecular weight of approximately 90 and is a united atom representation of a portion of the diblock urethane copolymer. Each ''soft segment'' monomer in the internodal chains of the polyurethane network corresponds to a butanediol chain extender $[HO-CH_2-CH_2-CH_2-CH_2-OH]$, whereas each toluene

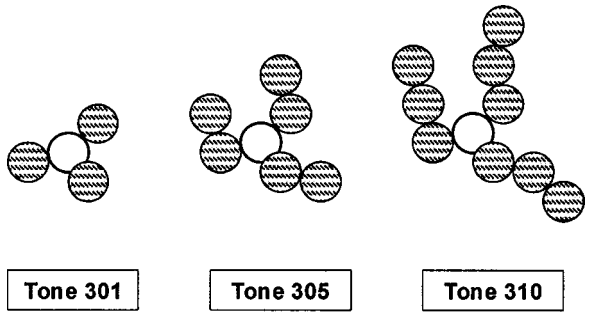

FIG. 1. Model soft segment structures for representation of cross-linking triols in the polyurethane block copolymer. Soft segment chains of varying length are appended to the trifunctional nodal segment in accordance with the class of Tone polymer selected.

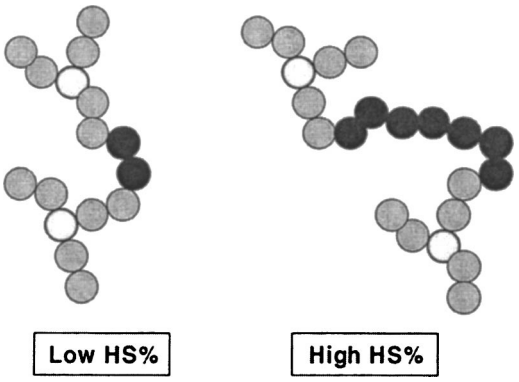

FIG. 2. Selection of hard segment weight fraction in model block copolymer network using hard segment chains of adjustable length to cross link trifunctional Tone polymer units.

diisocyanate $[CH_3(C_6H_3)(NCO)_2]$ molecule in the urethane copolymer is represented as an adjoining pair of "hard segment" monomer units.

The cross links in the simulated network are provided by trifunctional star polymers of varying chain length, as shown in Fig. 1. In the polyurethane block copolymer, these cross-linking agents are polycaprolactone-based triols, referred to by their trade name of Tone polymers. The Tone 301, Tone 305, and Tone 310 polymers have molecular weights of 300, 540, and 900, respectively, and are represented in the network model as three soft segment (hydroxyl-containing) chains connected to a single soft segment node. The sizes of the Tone 301, 305, and 310 triols are roughly approximated by using chain lengths of one, two, and three segments, respectively, for the star polymer arms.

Two types of networks were simulated. The first is a fully connected network, in which every Tone polymer nodal segment is cross linked to three neighboring nodal segments, and all cross links between nodes are the same length. A fully connected network of this type can be constructed by two methods. One approach is to assemble a diamond lattice of tetrafunctional nodes with fully extended cross links of the desired length, and delete one cross link for each pair of nodes, yielding a trifunctional network with uniform crosslinks. The disadvantage of this approach is that extensive, and therefore computationally costly, mechanical equilibration using slab moves is required to reduce the simulation cell to a volume that is representative of the density of polyurethane. An alternative method for generating the initial network structure that avoids this problem is to connect a lattice of nodes using ECCB-type moves to construct the cross-linking chains one segment at a time. The nodal spacing on the lattice is selected so that the target packing fraction for the network will be attained when all of the cross links have been assembled. Three cross links are then constructed for each node, using the ECCB algorithm to successively add freely jointed hard spherical segments to the growing chain so that closure of the cross link at the destination node occurs when the final segment is added. The hard segment weight fraction of the block copolymer network can be adjusted as shown in Fig. 2 by varying the number of hard segments in the bridging portion of the cross link between the Tone polymer soft segment arms.

Table I shows the details of the fully cross-linked model networks (Fxxx-xx) that were chosen for the simulations. In the fully connected networks, all cross links were the same length and contained the same number of hard and soft seg-

TABLE I. Summary description of model polyurethane networks. The network name encodes the Tone polymer type and the hard segment weight percentage (HS %) selected for each network, with "F" denoting a fully connected network, "P" denoting a partially cross-linked network, and "H" and "R" denoting fully connected networks with square-well ratios $\varepsilon_{ss}/\varepsilon_{hh}$ of 1 and 10 instead of the default value of 0.1. Also reported are the total number of segments N; the minimum, maximum, and mean lengths of the cross links L; and, for partially cross-linked networks, the minimum, maximum, and mean lengths of the dangling chains D.

Network	N	Tone	HS %	$\varepsilon_{ss}/\varepsilon_{hh}$	L_{avg}	L_{min}	L_{max}	D_{avg}	D_{min}	D_{max}
F301–50	1836	301	50	0.1	5	5	5	⋯	⋯	⋯
F301–65	2484	301	65	0.1	7	7	7	⋯	⋯	⋯
F305–17	1836	305	17	0.1	5	5	5	⋯	⋯	⋯
F305–50	928	305	50	0.1	9	9	9	⋯	⋯	⋯
F305–63	1216	305	63	0.1	12	12	12	⋯	⋯	⋯
F310–13	2484	310	13	0.1	7	7	7	⋯	⋯	⋯
F310–37	1024	310	37	0.1	10	10	10	⋯	⋯	⋯
F310–50	1312	310	50	0.1	13	13	13	⋯	⋯	⋯
P305–50	989	305	50	0.1	5.5	5	10	7.2	3	11
P310–38	1066	310	38	0.1	7.5	7	11	6.6	3	11
P310–50	1071	310	50	0.1	7.4	7	10	9.8	6	16
H310–50	1312	310	50	1	13	13	13	⋯	⋯	⋯
R310–50	1312	310	50	10	13	13	13	⋯	⋯	⋯

ments. The cross-link length was defined by the selection of the Tone polymer and the hard segment weight fraction. Specific model systems were constructed to facilitate comparison with experimental measurements of phase segregation in polyurethanes with known hard segment weight fraction and Tone polymer constituent.[5–7]

The second type of model network simulated was a partially cross-linked block copolymer network in which some of the nodal segments are cross linked to fewer than three other nodes. In this network type, the chain length between cross-linked nodes is also permitted to vary. To generate model structures for partially cross-linked networks, nodal segments were randomly distributed in the simulation cell, and the ECCB algorithm was used to extend three chain arms from each node, per the specifications of the Tone polymer size selected for the particular network. Next, hard segments were randomly appended to the ends of randomly selected chain arms. If two growing chain arms approached to within one segment diameter of one another, the two chain ends were repositioned so as to form a cross link between the two nodes associated with the chain arms. Chain growth and cross linking were then continued by sequentially adding more hard segments, until the desired hard segment weight fraction was achieved. The partially cross-linked networks were constructed so as to ensure that each chain contained at least one hard segment. The model networks (Pxxx-xx) obtained from this network generation algorithm are summarized in Table I, and contained nodes with fewer than three cross links and a segment length distribution for both the cross links and the dangling chains connected to only a single node.

Segment pairwise interactions in the model networks were simulated using the square-well potential

$$\begin{aligned} U(r_{ij}) &= \infty, \quad r_{ij} < \sigma \\ &= -\varepsilon_{ij}, \quad \sigma \leqslant r_{ij} \leqslant \lambda\sigma \\ &= 0, \quad \lambda\sigma \leqslant r_{ij}, \end{aligned} \tag{1}$$

where r_{ij} is the distance between the centers of segments i and j, σ is the segment diameter, $(\lambda-1)\sigma$ is the square-well width, and ε_{ij} is the square-well depth for the interaction of segments i and j. Interactions between covalently bonded segments and between second-nearest neighbors (i.e., two segments that are bonded to a common third segment) on polymer chains are excluded from the potential summation. In this simulation study, $\lambda=1.5$ and the diameters of the hard and soft segments are the same. For the diblock copolymer network there are three different square-well depth parameters that describe the interaction energy between two hard segments, two soft segments, and a hard and a soft segment. In the case of the polyurethane system, the largest of the three pairwise interaction terms is expected to be the hard segment pair interaction, since it is the interactions of the hard segments on neighboring cross links which leads to phase segregation of polyurethane matrices.[5] Therefore, the potential in Eq. (1) is scaled with respect to the square-well depth for hard segment pairs ε_{hh} to express the energy of the system in a dimensionless form. In relation to the polyurethane block copolymer, the segment diameter and hard segment pair square-well depth can be estimated as $\sigma \sim 5$ Å and $\varepsilon_{hh}/k_B \sim 400$ K, respectively, from comparison with square-well parameters for *n*-butane and benzene, two significant components of the carbon backbone of polyurethane.

For most of the networks modeled in Table I, the square-well depth for interactions between pairs of soft segments was assigned a value one-tenth of the hard segment pair square-well depth; i.e., $\varepsilon_{ss}/\varepsilon_{hh}=0.1$. The Lorentz–Berthelot mixing rule was invoked to assign the square-well depth of the hard segment/soft segment pair interaction as the geometric mean of the well depths for same segment pairs: $\varepsilon_{hs}=(\varepsilon_{hh}\varepsilon_{ss})^{1/2}$. For two of the networks listed in Table I, the soft segment pair square-well depth was modified to examine the effect of this parameter on the network structure. For the homopolymer (H310–50), $\varepsilon_{ss}/\varepsilon_{hh}=1$ so that all segments in this network are energetically indistinguishable from one another. For network R310–50, the relative magnitudes of the same segment square-well depths are reversed ($\varepsilon_{ss}/\varepsilon_{hh}=10$) so that the soft segment pairs have the largest interaction energy rather than the hard segment pairs.

For all of the model networks, isobaric–isothermal Monte Carlo simulations were conducted using periodic boundary conditions to simulate bulk behavior. As previously noted, ECCB and slab moves were used to equilibrate the network from its initial configuration. No breaking of bonds or formation of new bonds between segments was permitted, and a constant bond distance of σ was maintained between all covalently bonded segments. Otherwise, all segments, including nodes, were allowed to move as freely jointed segments, and no lattice constraints were imposed.

The NPT MC simulations were run at 373 K and 1 atm, corresponding to the temperature and pressure at which polyurethane curing is commonly performed.[5] All systems were initially equilibrated with a ratio of ECCB to slab (volume sampling) moves of 1:1. As the packing fraction and potential energy of the system approached their equilibrium values, the ratio of ECCB moves to slab moves was gradually increased to 10 000:1 to allow more efficient sampling of the configuration space. Equilibration and statistical sampling of a single model network typically required 1.5×10^8 ECCB moves and 3×10^5 slab moves.

Configurational snapshots of equilibrated network structures were prepared using IRIS Explorer visualization software. While the snapshots provide a useful visual tool in assessing whether phase segregation has occurred in a network, a more quantitative measurement is desired to make this determination. Radial distribution functions (RDFs) serve this purpose. For polymer segments that interact with spherical potentials (e.g., the square-well potential), the RDF characterizes the relative structure of the network that arises due to correlation between pairs of segments. Values of the radial distribution function $g_{ij}(r)=1$ indicate no correlation between segment types i and j at a given distance r, whereas if $g_{ij}(r)>1$ then there is an enhanced probability of finding the two segments separated by that distance, and if $g_{ij}(r)<1$ the probability is decreased for that separation. For block copolymer networks that phase segregate, one therefore expects that the RDFs for same segment pairs, $g_{hh}(r)$ and $g_{ss}(r)$, will exhibit peak values for separation distances cor-

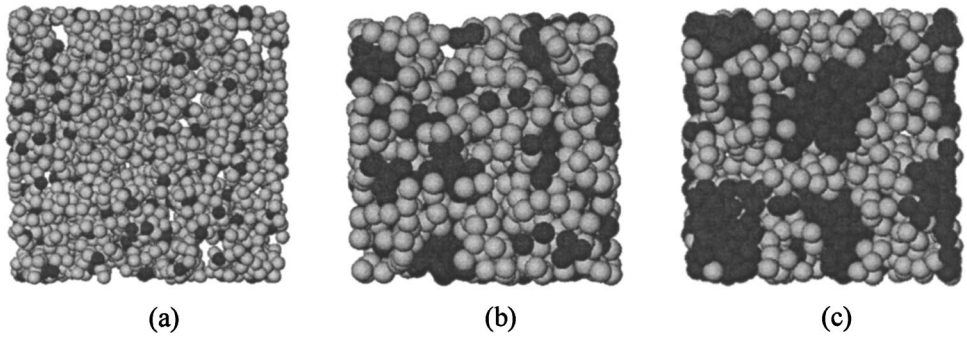

FIG. 3. Configurational snapshots of equilibrated Tone 310 networks with hard segment weight fractions of (a) 0.13; (b) 0.37; and (c) 0.50. The light-shaded spheres are the soft segments of the block copolymer, and the dark-shaded spheres are the hard segments.

responding to the square-well interaction; i.e., $g_{hh}(r)$ and $g_{ss}(r)>1$ for $\sigma \leqslant r \leqslant \lambda\sigma$. Conversely, one anticipates that unlike segments will be excluded from this separation distance: $g_{hs}(r)<1$ for $\sigma \leqslant r \leqslant \lambda\sigma$. RDFs were therefore compiled in bin increments of 0.05 σ using standard histogram techniques[44] for pairs of hard segments, pairs of soft segments, and hard segment/soft segment pairs, so that the extent of phase segregation in the network could be evaluated by nonvisual means. Covalently bonded segments were excluded from the RDF compilations since these segments are constrained to have a fixed separation distance of σ. For brevity, the radial distribution functions $g_{hh}(r)$, $g_{ss}(r)$, and $g_{hs}(r)$ are hereafter referred to as the hard–hard, soft–soft, and hard–soft RDFs, respectively.

III. RESULTS AND DISCUSSION

The set of model networks in Table I was selected so that the hard segment weight fraction, cross-link length, and degree of connectivity could be independently varied and their effects evaluated on the phase segregation of the block copolymer network. A summary follows of the observed effect of each of these structure parameters on the phase segregation behavior of the model polyurethane networks.

A. Hard segment weight fraction

The fractional hard segment content of the polymer network was varied for the same Tone polymer (soft segment) cross-linking agent in three sequences of fully cross-linked model structures: F301–50/F301–65 for networks containing Tone 301; F305–17/F305–50/F305–63 for Tone 305 networks; and F310–13/F310–37/F310–50 for Tone 310 networks. Configurational snapshots of equilibrated structures for the Tone 310 network sequence are shown in Fig. 3. From perusal of these snapshots it is evident that little association of hard segments occurs in network F310–13, whereas sizable hard segment domains have established within F310–50, the Tone 310 network with the highest hard segment weight fraction. For F310–37, it is difficult to ascertain from inspecting viewgraphs whether this network is phase segregated. Hence, the RDFs for hard–hard, soft–soft, and hard–soft segment pairs are consulted to make this determination. The RDFs obtained for the three equilibrated Tone 310 networks are shown in Figs. 4, 5 and 6, respectively, for the 13, 37, and 50 weight percent hard segment structures. There are several common features of the RDFs irrespective of the segment pair type or network structural parameters. For $r<\sigma$, $g(r)=0$ for all pair correlations due to the hard sphere repulsion part of the square-well potential. The cutoff of the attractive portion of the square-well potential at $r=1.5\sigma$ gives rise to discontinuities in the RDFs at this separation distance as well. Finally, as required the RDFs trend toward a value of unity at large separation distances, where segment pairs become structurally uncorrelated.

Closer inspection of the RDFs in the range of separation distances corresponding to the square-well attraction ($\sigma \leqslant r \leqslant 1.5\sigma$) reveals distinctions between the hard–hard, soft–soft, and hard–soft pair correlation functions as the hard segment fraction of the network is varied. For the network with the low weight percentage of hard segments, F310–13, the

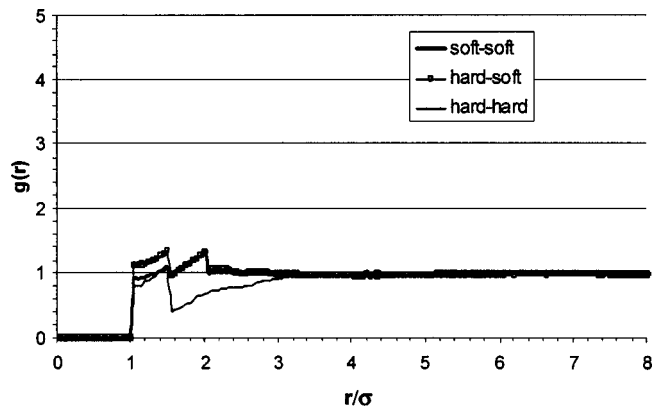

FIG. 4. Radial distribution functions for segment pairs in network F310–13.

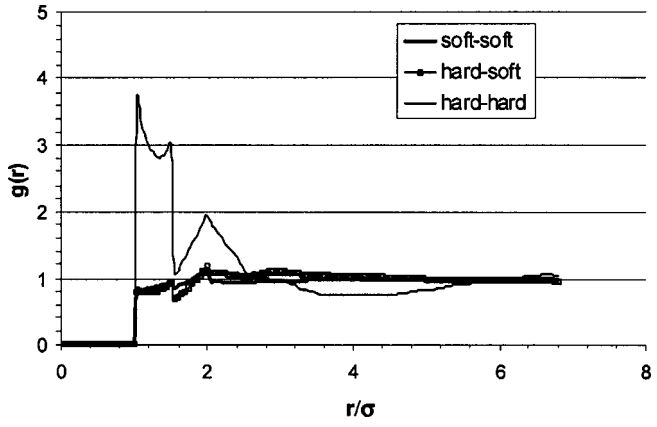

FIG. 5. Radial distribution functions for segment pairs in network F310–37.

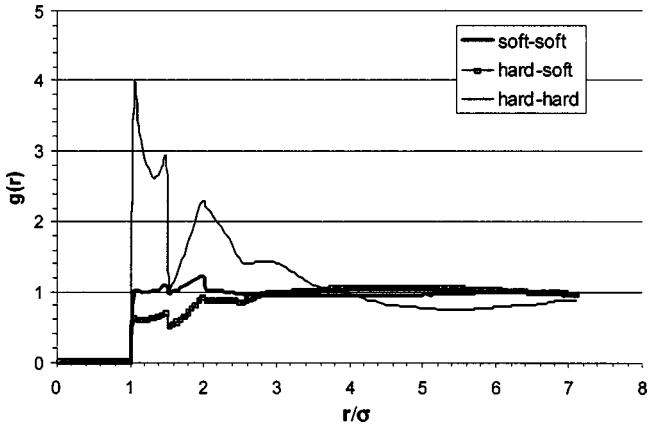

FIG. 6. Radial distribution functions for segment pairs in network F310–50.

RDFs for the three types of segment pairs are nearly indistinguishable over this separation range, indicating that there are no short-range structural correlations between same-segment pairs and therefore no phase segregation. For network F310–50, by contrast, the large peak in $g_{hh}(r)$ in the square-well range confirms that this network is strongly phase segregated into hard segment and soft segment domains. The existence of the latter domains is indicated by the deselection of unlike segment pairs in the square-well range of the RDF; i.e., $g_{hs}(r)<1$ at short range. For the F310–37 network, the soft–soft and hard–soft RDFs are indistinguishable, so there is no observed preference for soft segments to congregate with other soft segments. However, the $g_{hh}(r)$ correlation shows there is clearly a preference for hard segments on neighboring chains to form subdomains within the structure. On the basis of the segment pair RDFs, it is therefore inconclusive whether this network can be classified as phase segregated. One might reasonably adopt, as a condition of phase segregation, that both types of segments, hard and soft, form same-segment subdomains. By this standard, F310–37 would not be considered a phase-segregated network.

The effect of the hard segment weight fraction was also investigated for fully cross-linked networks constructed from the Tone 301 and Tone 305 polymers. No phase segregation was observed in either of the Tone 301 networks, F301–50 and F301–65. The RDFs and a configurational snapshot for the F301–50 network are shown in Fig. 7; similar correlation functions were obtained for F301–65. Since $g_{hs}(r)$ lies intermediate between $g_{hh}(r)$ and $g_{ss}(r)$ in the range of distances corresponding to the square-well attraction, these networks do not appear to be phase segregated. RDF analysis of the three Tone 305 networks yielded similar results as for the Tone 310 structures: for high hard segment weight percentages (50% and 63%) the Tone 305 networks phase segregated, while at low hard segment weight percentage (17%) no phase segregation occurred. The RDFs for these networks mirror the respective correlations presented as a function of hard segment content for the Tone 310 networks in Figs. 4–6, and so for brevity the Tone 305 RDFs are not shown.

B. Crosslink length

In the preceding analysis of the effect of the hard segment weight fraction on phase segregation, the cross-link length increased as the weight percentage of hard segments increased within a Tone polymer family. In order to differentiate between the effects of the cross-link length and the hard segment content, another three sets of fully cross-linked model structures were examined in which the chain arm length of the Tone polymer used to cross link the network was varied while the hard segment weight fraction was held constant (or nearly constant). These sequences are: F305–17/F310–13 (~15% hard segments by weight); F301–50/F305–50/F310–50 (50% hard segments); and F301–65/F305–63 (~64% hard segments).

Configurational snapshots and RDFs for several of these networks have been presented in Figs. 4–7 and do not require additional elaboration. It is observed from the simulations that the propensity of the network to phase segregate increases as the Tone polymer size increases. The F301–50 network, for example, does not phase segregate, whereas the F305–50 and F310–50 networks are both definitively phase segregated. Since all three of these networks are composed of 50% hard segments, it is apparent that the hard segment content is not the sole determinant of the phase segregation behavior of the model networks. In the case of the 50% hard segment networks, as the Tone polymer size is increased, parity between the total number of hard segments and soft

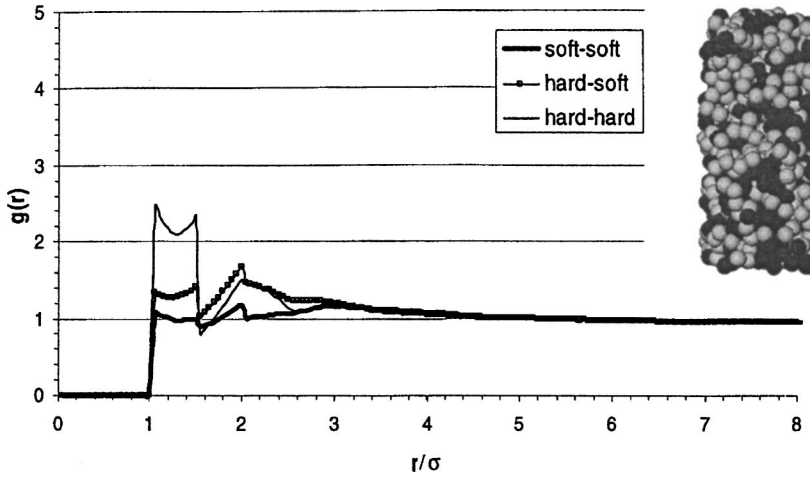

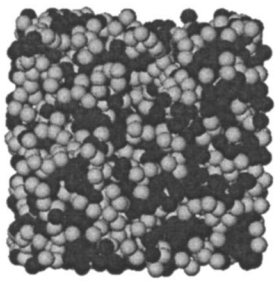

FIG. 7. Radial distribution functions for segment pairs in network F301–50. The inset shows a snapshot of the equilibrated network structure.

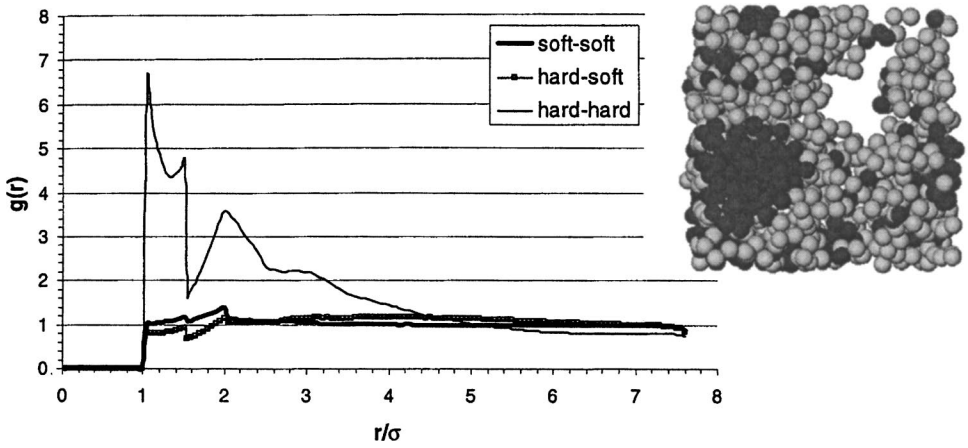

FIG. 8. Radial distribution functions for segment pairs in network P310–38. The inset shows a snapshot of the equilibrated network structure.

segments is maintained by extending the length of hard segment bridges that cross link the Tone polymer chain arms. Hence, the total cross-link length from node to node in these networks increases from five segments for the F301–50 network, to 9 and 13 segments, respectively, for the F305–50 and F310–50 networks, even as the hard segment weight fraction is held constant. For networks with short cross links, the connectivity constraints are severe, and so there is limited opportunity for hard segments and soft segments to phase segregate into separate domains. For networks with longer cross links, steric hindrances are reduced and the cross-linking chains can more freely configure themselves so as to maximize their nonbonded energetic interactions with segments on neighboring chains. For the fully connected networks studied, the critical cross-link length for phase segregation appears to be about nine or ten segments, although having cross links present of this size does not necessarily guarantee that phase segregation will occur. For example, the F305–50 network with $L=9$ is unambiguously phase segregated, whereas the F310–37 network with $L=10$ does not phase segregate. It is apparent that other factors, such as the hard segment content and the square-well potential parameter values, also influence whether phase segregation occurs in a given network structure. In general, however, it can be concluded that sufficiently heterogeneous diblock copolymer networks (i.e., those that contain significant hard segment content) will phase segregate to a greater extent as the Tone polymer chain length is increased.

C. Connectivity

Three partially cross-linked networks were constructed that have Tone polymer size and hard segment weight fractions that are either identical or nearly the same as fully connected networks in Table I. The partially cross-linked structures, and their fully connected analogs, are P305–50/F305–50; P310–38/F310–37; and P310–50/F310–50. By comparing the equilibrated structures of the partially cross-linked networks to their fully connected equivalents, the effect of connectivity on phase segregation can be assessed. This is particularly important for any implications that are to be drawn from the simulation results concerning the phase segregation of polyurethane block copolymer networks, since the process of reaction injection molding[5] by which the polyurethane matrices are formed likely yields partially cross linked rather than fully interconnected network structures.

Figure 8 shows the segment pair RDFs and a configurational snapshot of the equilibrated structure of network P310–38. By virtue of its method of generation, the structure of this network is more irregular than the fully connected networks previously discussed, with polydispersity in the lengths of both the cross-linking chains and the dangling chain ends of P310–38 (see Table I). Phase segregation is visually identifiable in the snapshot of Fig. 8, and the pair correlation functions confirm that this segregation spans the network. In comparing the RDFs of the partially cross-linked network in Fig. 8 with the RDFs of the fully connected structure analog F310–37 in Fig. 5, it can be seen that the square-well peak of the hard segment pair RDF is markedly enhanced in the partially cross-linked structure relative to the fully connected network. Also, a slight but distinct increase in $g_{ss}(r)$ relative to $g_{hs}(r)$ occurs in the square-well range for network P310–38, whereas for F310–37 these same two RDFs are nearly indistinguishable. If formation of soft segment domains as well as hard segment domains is a signatory feature of network phase segregation, then this difference in the RDFs takes on added significance.

A large increase in phase segregation was also observed in the P305–50 network relative to the F305–50 network, and a modest increase in P310–50 relative to F310–50. Presumably, the dangling chain ends of the partially cross-linked structures enable these networks to more freely sample the available configuration space, and hence they more readily form hard segment and soft segment subdomains. This leads to increased phase segregation of partially cross-linked networks such as P310–38 relative to fully connected networks like F310–37, even though the average cross-link length in P310–38 is several segments shorter than in F310–37. Lower connectivity is therefore seen to impart a greater likelihood of phase segregation in the model copolymer networks. This finding should be kept in mind in using molecular simulations to evaluate phase segregation of polyurethanes, as the results from simulations of fully con-

nected block copolymer networks are likely to underestimate the extent of phase segregation that actually occurs in the partially cross-linked polyurethane matrices.

D. Square-well ratio

The F310–50, H310–50, and R310–50 networks are identical in all respects save for the magnitude of the square-well depths for the hard segment pairs and soft segment pairs. H310–50 is a homopolymer in which the hard segment and soft segments are identified in name only, as the hard–hard, soft–soft, and hard–soft pairwise interactions are energetically indistinguishable. Predictably, no phase segregation occurs in this network. The structure correlations for this network are not shown, but the only notable feature of the H310–50 RDFs is that $g_{hh}(r)$ shows a slightly higher peak in the square-well region than the other two pair correlation functions. This difference is ascribed to the fact that the hard segments on the bridging cross links have exactly two bond constraints per segment, whereas the average number of bond constraints per soft segment is slightly greater than two due to the presence of the trifunctional soft segment nodes. Thus, the hard segments have somewhat more freedom than the soft segments, on average, to sample the configuration space and maximize square-well interactions with neighboring segments. This effect is small, however, and a substantive difference in energetic interactions between hard segment and soft segment pairs is required in order for the model networks to phase segregate.

When the square well ratio $\varepsilon_{ss}/\varepsilon_{hh}$ is inverted from 0.1 (for F310–50) to 10 (for R310–50) for the Tone 310 polymer with 50% hard segments, the network still phase segregates. However, the nature of the phase segregation changes, as one might expect. For the R310–50 network, the formation of soft segment domains is energetically most favored, and so the square-well peak for $g_{ss}(r)$ for this network greatly exceeds that for $g_{hh}(r)$. The RDFs (not shown) are essentially the same as those shown in Fig. 6, with the hard–hard and soft–soft RDFs interchanged and the hard–soft correlation again deselected in the square-well region. The effect of the square-well ratio on the network structure can be observed from inspection of Fig. 9, which shows selected fragments of the equilibrated F301–50 and R301–50 networks with the nodal segments highlighted. For the network with $\varepsilon_{ss}/\varepsilon_{hh}=0.1$ [Fig. 9(a)], the nodal segments are spaced relatively far apart in order to accommodate formation of hard segment domains, whereas for the network with $\varepsilon_{ss}/\varepsilon_{hh}=10$ [Fig. 9(b)], nodal segment pairs are in close contact so as maximize potential interactions between soft segments on the Tone polymer chains. The structural differences of the F301–50, R301–50, and H301–50 (homopolymer) networks are neatly encapsulated in the node–node RDFs reported in Fig. 10. Because the nodal segments are a small subset of the total network of polymer segments, the statistics for the RDFs in Fig. 10 are less well-developed than in the previous RDFs shown. However, it can clearly be confirmed from inspection of the RDFs that the square-well ratio exerts a profound influence on the node–node correlation, and by extension the phase segregation behavior of the network itself. For square-well ratios that exceed unity, the network structure forms around soft segment domains in the vicinity of the nodes, while for $\varepsilon_{ss}/\varepsilon_{hh}$ ratios less than unity, hard segment domains in the bridging cross links dictate the network structure.

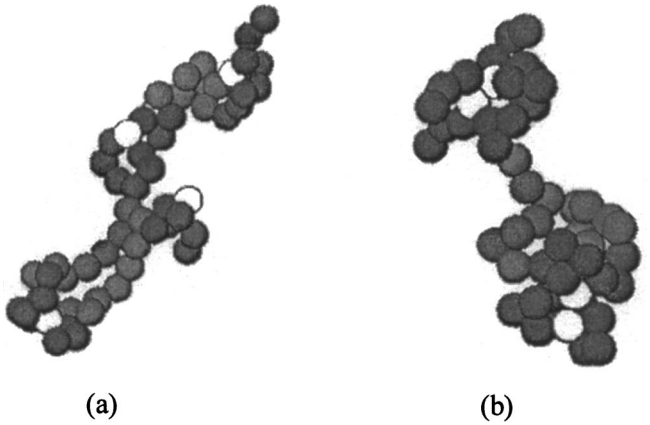

FIG. 9. Configurational snapshots of portions of the equilibrated (a) F310–50 and (b) R310–50 networks showing effect of square-well ratio for soft segment pairs and hard segment pairs on cross-link structure. The light- and dark-shaded spheres in each snapshot are hard segments and soft segments, respectively. The unshaded spheres are the trifunctional nodal segments.

E. Comparison to experimental polyurethane networks

Table II summarizes the observed phase segregation behavior for the 13 model block copolymer networks described in Table I. A comparison to differential scanning calorimetry measurements of phase segregation in experimental polyurethane networks[5] with Tone size and hard segment content similar to those of the model networks is also presented in Table II, along with previously reported Flory theory predictions[6] for phase segregation in these matrices. In some cases the comparison of the simulation and experimental results is approximate, since the hard segment weight fractions of the two networks do not precisely match. Nonetheless, where such comparisons can be drawn, it can be seen that the molecular simulation results accurately predict the phase segregation outcome. For the case of Tone 310 polyurethane with 38% hard segments, it should be noted that the phase

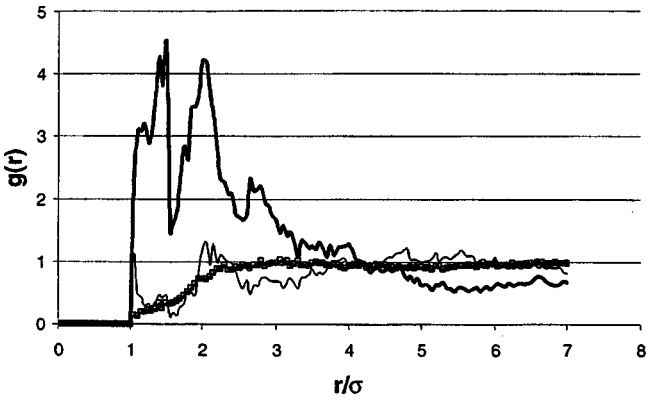

FIG. 10. Radial distribution functions for node pairs in networks F310–50 (squares), H310–50 (thin line), and R310–50 (thick line).

TABLE II. Predicted phase segregation from molecular simulation (this work) and from Flory theory (Ref. 6) for model block copolymer networks, and experimental observations (Ref. 5) of phase segregation for polyurethane networks with comparable Tone polymer chain length and hard segment weight fraction.

Polyurethane		Phase segregated?			Model network
Tone	HS %	Experiment	Flory theory	Simulation	
301	43	no	no	⋯	⋯
	57	no	no	no	F301–50
	64	no	no	no	F301–65
305	33	no	no	no	F305–17
	44	no	yes	⋯	⋯
	57	yes	yes	yes	F305–50
	⋯	⋯	⋯	yes	P305–50
	65	yes	yes	yes	F305–63
310	23	no	no	no	F310–13
	38	no	yes	no	F310–37
	⋯	⋯	⋯	yes	P310–38
	48	maybe	yes	⋯	⋯
	52	yes	yes	yes	F310–50
	⋯	⋯	⋯	yes	P310–50
	⋯	⋯	⋯	no	H310–50
	⋯	⋯	⋯	yes	R310–50
	67	yes	yes	⋯	⋯

segregation observed in the experiment does not occur in the fully connected model network F310–37, but it does occur in the partially cross-linked network P310–38. The Flory theory meanwhile correctly predicts the experimental outcome in all but two of the test cases, with a third result (Tone 310, 48% hard segments) deemed inconclusive on account of indeterminate experimental results.

IV. SUMMARY AND CONCLUDING REMARKS

From configurational bias Monte Carlo simulation, it has been established that phase segregration in diblock copolymer networks with trifunctional cross-linking nodes is favored by the following conditions, in perceived decreasing order of importance: (1) a large difference in the well depth energies ϵ_{ss} and ϵ_{hh} for the interactions of soft segment pairs and hard segment pairs; (2) longer cross-link length (e.g., a high molecular weight Tone polymer constituent); (3) higher hard segment weight fraction; and (4) lower connectivity (i.e., partial rather than full cross linking of the network). The simulations confirm trends observed in experimental measurements of phase segregation in which the Tone polymer was substituted or the hard segment content was varied, even though no attempt was made to fit the square-well potential parameters of the model to experimental data. Further refinements of the model by parameter fitting, or by using a soft-sphere potential with flexible bonds and bond angle constraints, are therefore possible. Additionally, the cross-link length and connectivity of the network may be more carefully tailored to experimental data to improve realism. In conclusion, the model networks and configurational bias Monte Carlo methods employed in this work can be used to confidently predict the phase segregation behavior of polyurethanes and other block copolymer materials, given the composition of the polymer constituents and the mode of cross linking of the network.

ACKNOWLEDGMENTS

We gratefully acknowledge the Michigan State University Composite Materials and Structures Center for support of this research. The authors thank Fernando Escobedo (Cornell University) and Juan de Pablo (University of Wisconsin) for providing FORTRAN source codes for the ECCB and slab algorithms.

[1] J. R. Dawson and J. B. Shortall, Cellular Polymers **1**, 41 (1982).
[2] C. Kau, A. Hiltner, E. Baer, and L. Huber, J. Reinf. Plast. Compos. **8**, 18 (1989).
[3] E. G. Schwarz, F. E. Critchfield, L. P. Tackett, and P. M. Tarin, J. Elastomers Plastics **11**, 280 (1979).
[4] P. C. Yang and W. M. Lee, J. Elastomers Plastics **19**, 120 (1987).
[5] R. K. Agrawal and L. T. Drzal, J. Adhes. **54**, 79 (1995).
[6] R. K. Agrawal and L. T. Drzal, J. Adhes. Sci. Technol. **9**, 1381 (1995).
[7] R. K. Agrawal and L. T. Drzal, J. Adhes. **55**, 221 (1996).
[8] C. W. Macosko, *RIM Fundamentals of Reaction Injection Molding* (Hanser, New York, 1989).
[9] J. G. Eberhart, J. Phys. Chem. **70**, 1183 (1966).
[10] D. W. Van Krevelen, *Properties of Polymers*, 3rd ed. (Elsevier Science, New York, 1990).
[11] *Monte Carlo and Molecular Dynamics Simulations in Polymer Science*, edited by K. Binder (Oxford University Press, New York, 1995).
[12] E. R. Duering, K. Kremer, and G. S. Grest, Phys. Rev. Lett. **67**, 3531 (1991).
[13] G. S. Grest and K. Kremer, J. Phys. (Paris) **51**, 2829 (1990).
[14] G. S. Grest and K. Kremer, Macromolecules **23**, 4994 (1990).
[15] S. Lay, J. Sommer, and A. Blumen, J. Chem. Phys. **110**, 12173 (1999).
[16] M. Plischke and S. J. Barsky, Phys. Rev. E **58**, 3347 (1998).
[17] M. Schulz and J. U. Sommer, J. Chem. Phys. **96**, 7102 (1992).
[18] J. U. Sommer, Macromol. Symp. **81**, 139 (1994).
[19] J. U. Sommer, M. Schulz, and H. L. Trautenberg, J. Chem. Phys. **98**, 7515 (1993).
[20] E. R. Duering, K. Kremer, and G. S. Grest, Macromolecules **26**, 3241 (1993).
[21] E. R. Duering, K. Kremer, and G. S. Grest, J. Chem. Phys. **101**, 8169 (1994).
[22] G. S. Grest, K. Kremer, and E. R. Duering, Europhys. Lett. **19**, 195 (1992).
[23] G. S. Grest, K. Kremer, and E. R. Duering, Physica A **194**, 330 (1993).

[24] N. R. Kenkare, C. K. Hall, and S. A. Khan, J. Chem. Phys. **110**, 7556 (1990).
[25] N. R. Kenkare, S. W. Smith, C. K. Hall, and S. A. Khan, Macromolecules **31**, 5861 (1998).
[26] T. Hölzl, H. L. Trautenberg, and D. Göritz, Phys. Rev. Lett. **79**, 2293 (1997).
[27] H. L. Trautenberg, J. U. Sommer, and D. Göritz, J. Chem. Soc., Faraday Trans. **91**, 2649 (1995).
[28] F. A. Escobedo and J. J. de Pablo, J. Chem. Phys. **104**, 4788 (1996).
[29] F. A. Escobedo and J. J. de Pablo, Mol. Phys. **90**, 437 (1997).
[30] F. A. Escobedo and J. J. de Pablo, J. Chem. Phys. **106**, 793 (1997).
[31] F. A. Escobedo and J. J. de Pablo, J. Chem. Phys. **102**, 2636 (1995).
[32] F. A. Escobedo and J. J. de Pablo, Macromol. Theory Simul. **4**, 691 (1995).
[33] P. J. Flory, *Principles of Polymer Chemistry* (Cornell University Press, Ithaca, NY, 1953).
[34] S. K. Nath, J. D. McCoy, J. G. Curro, and R. S. Saunders, J. Polym. Sci., Part B: Polym. Phys. **33**, 2307 (1995).
[35] H. Benoit and G. Hadziioannou, Macromolecules **21**, 1449 (1988).
[36] P. G. De Gennes, J. Phys. (Paris) **40**, 69 (1979).
[37] E. Vargas and M. C. Barbosa, Physica A **257**, 312 (1998).
[38] N. Metropolis, A. W. Rosenbluth, M. N. Rosenbluth, A. H. Teller, and E. Teller, J. Chem. Phys. **21**, 1087 (1953).
[39] M. N. Rosenbluth and A. W. Rosenbluth, J. Chem. Phys. **23**, 356 (1955).
[40] J. I. Siepmann and D. Frenkel, Mol. Phys. **75**, 59 (1992).
[41] J. J. De Pablo, M. Laso, and U. W. Suter, J. Chem. Phys. **96**, 2395 (1992).
[42] S. K. Kumar, M. Vacatello, and D. Y. Yoon, J. Chem. Phys. **89**, 5206 (1988).
[43] X. Li and Y. C. Chiew, J. Chem. Phys. **101**, 2522 (1994).
[44] R. L. Rowley, *Statistical Mechanics for Thermophysical Property Calculations* (Prentice Hall, Englewood Cliffs, NJ, 1994).